Integrated Mach-Zehnder Interferometer : Theory, Design, Fabrication and Analysis

Sarath K T, *Traana Technologies, India*

***Abstract*—MachZehnder Interferometer is a widely used component in photonics for modulation, switching, filtering and sensing. The design adapted to MachZehnder modulator can be used in realizing various analog and digital communication modulations. Integrated Photonics focus on miniaturization of photonic components and circuits in chip level. When this is done using Silicon, it becomes Silicon Photonics technology. Hence it is very important to know the theory, design, and fabrication of Mach Zehnder Interferometer. This paper focus on these topics along with the analysis of experimental results and simulation results.**

***Index Terms*—Integrated Photonics, Silicon on Insulator, Mac-Zehnder Interferometer**

I. INTRODUCTION

Integrated Photonics is the science of miniaturization of photonic components in chip scale. But these requires careful design methodologies and fabrication process than bulk photonic modules. Silicon has been a popular choice for Integrated Photonics due to its mature micro/nano technologies in electronics. Hence Silicon Photonics has become a center of attraction.

Mach Zehnder Interferometer (MZI) works on the principle of interference. This is one of the important components used in a wide variety of photonic applications. The design, extended to Mach Zehnder Modulator (MZM) finds in a variety of applications including Optical Communication [1], Bio-Photonic sensing [2], Microwave Photonics [3] etc.

II. THEORY

Mach Zehnder Interferometer (MZI) consist of a splitter which splits the light into two waveguides. These then gets combined at the combiner. Depending on the phase difference between these waveguides, the outputs is either constructively or destructively or in between. When the two waveguides are of equal length, the MZI is said to be in balanced configuration and if there is a difference in length, it is said to be in unbalanced configuration.

A typical MZI is as shown in Fig 1, where the top arm has length L and bottom arm has length L+ ΔL. Optical Source is usually a laser and optical detector can be Photodiode or Avalanche Photodiode.

First Author. Sarath K T is with Traana Technologies, India (e-mail: sarath@traana.in / ktsarath40@gmail.com.)

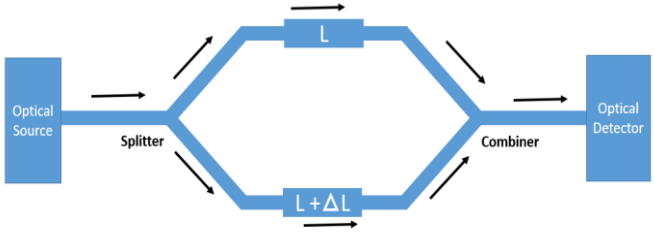

Fig. 1. Mach Zehnder Interferometer with optical source and detector

A. Modelling and Simulation of Modal Profiles using MODE

The modal profile analysis is done using Lumerical MODE solutions. Through these simulations one can obtain the effective index and group index of waveguides.

The model profile of TE waveguide is simulated using Eigen Mode Solver. The energy density of quasi-TE mode is as shown in Fig 2.

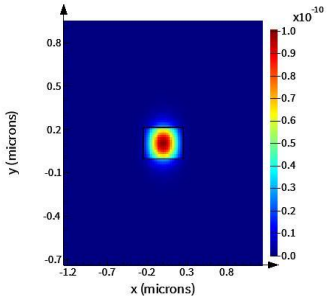

Fig. 2. Energy density of quasi-TE mode

Various other components of the modal profile can be extracted, one of which is the x component of the Electric Field is as shown in Fig 3.

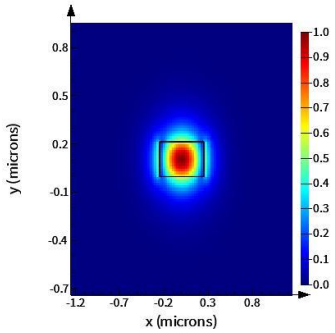

Fig. 3. Ex component of quasi-TE mode

Effective index variation is plotted v/s wavelength which is spanned from 1500 nm to 1600 nm. This is as shown in Fig 4.

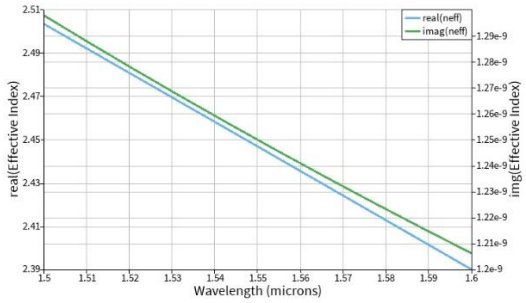

Fig. 4. Effective Index Variation with respect to wavelength

The group index variation with respect to wavelength is also extracted using the standard simulation software and the variation is as shown in Fig 5.

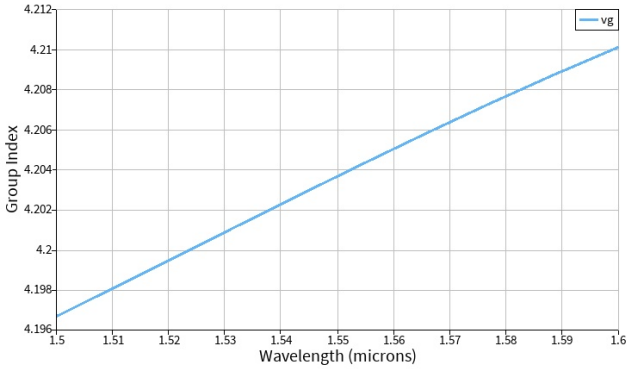

Fig. 5. Group Index Variation with respect to wavelength

Wavelength compact model is derived for the waveguide. This essentially is a second order polynomial and the coefficients are derived using a matlab script. The result is as shown in Fig 6.

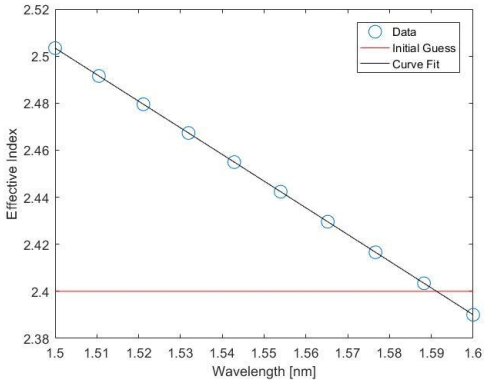

Fig. 6. Compact model of the TE mode, in terms of the effective index

B. MZI Modelling using INTERCONNECT

Using INTERCONNECT, MZI is modelled and then analyzed for its FSR and transmission spectra.
The TE gain of the MZI is extracted and shown in Fig 7.

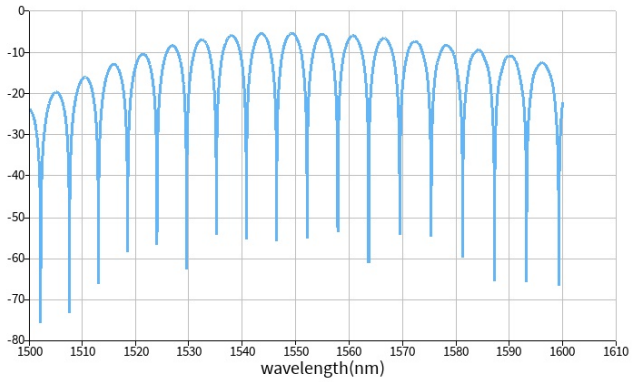

Fig. 7. TE gain with MZI (including grating coupler)

The Free Spectral Range (FSR) is extracted and is as shown in Fig 8.

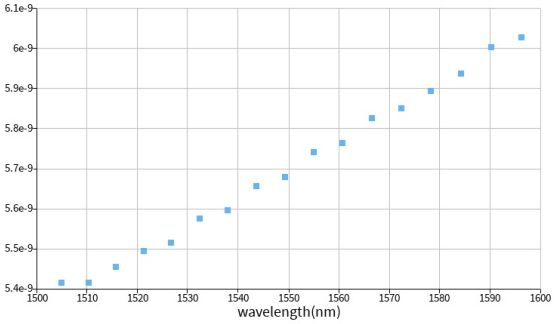

Fig. 8. FSR of MZI with respect to wavelength

II. LAYOUT USING KLAYOUT

The Layout is done in KLOUT software and using the SiEPIC PDKs. The draft Layout is as shown in Fig 9.
The top row corresponds to TE mode profiles in which the first one is for reference or de-embedding. The length variation from structures 2 to 4 are 38.52 um, 74 um, 200.6 respectively. In order to check the manufacturing repeatability, the dimension of 4 and 5 is kept the same.

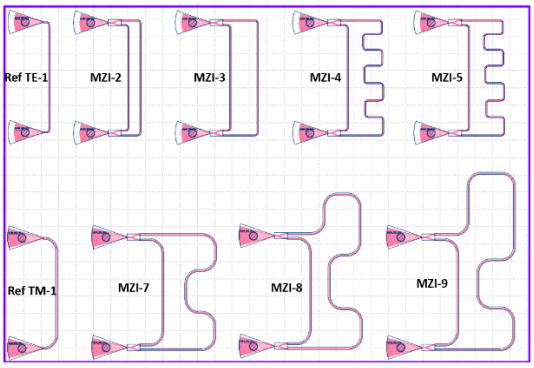

Fig. 9. KL Layout with length 605 um and width 410 um

The bottom row is maintained for TM mode profiles in which the first structure is for referencing. Structures 7-9 corresponds to length differences of 174 um, 253.2 um and 327 um respectively.

III. Fabrication

The photonic devices were fabricated using the NanoSOI MPW fabrication process by Applied Nanotools Inc. (http://www.appliednt.com/nanosoi; Edmonton, Canada) which is based on direct-write 100 keV electron beam lithography technology. Silicon-on-insulator wafers of 200 mm diameter, 220 nm device thickness and 2 µm buffer oxide thickness are used as the base material for the fabrication. The wafer was pre-diced into square substrates with dimensions of 25x25 mm, and lines were scribed into the substrate backsides to facilitate easy separation into smaller chips once fabrication was complete. After an initial wafer clean using piranha solution (3:1 H2SO4:H2O2) for 15 minutes and water/IPA rinse, hydrogen silsesquioxane (HSQ) resist was spin-coated onto the substrate and heated to evaporate the solvent. The photonic devices were patterned using a JEOL JBX-8100FS electron beam instrument at The University of British Columbia. The exposure dosage of the design was corrected for proximity effects that result from the backscatter of electrons from exposure of nearby features. Shape writing order was optimized for efficient patterning and minimal beam drift. After the e-beam exposure and subsequent development with a tetramethylammonium sulfate (TMAH) solution, the devices were inspected optically for residues and/or defects. The chips were then mounted on a 4" handle wafer and underwent an anisotropic ICP-RIE etch process using chlorine after qualification of the etch rate. The resist was removed from the surface of the devices using a 10:1 buffer oxide wet etch, and the devices were inspected using a scanning electron microscope (SEM) to verify patterning and etch quality. A 2.2 µm oxide cladding was deposited using a plasma-enhanced chemical vapour deposition (PECVD) process based on tetraethyl orthosilicate (TEOS) at 300ºC. Reflectrometry measurements were performed throughout the process to verify the device layer, buffer oxide and cladding thicknesses before delivery

III. EXPERIMENTAL DATA AND ANALYSIS

A. Measurement Description

To characterize the devices, a custom-built automated test setup [4, 8] with automated control software written in Python was used [5]. An Agilent 81600B tunable laser was used as the input source and Agilent 81635A optical power sensors as the output detectors. The wavelength was swept from 1500 to 1600 nm in 10 pm steps. A polarization maintaining (PM) fibre was used to maintain the polarization state of the light, to couple the TE polarization into the grating couplers [4]. A 90º rotation was used to inject light into the TM grating couplers [6]. A polarization maintaining fibre array was used to couple light in/out of the chip [7].

B. Manufacturing Challenges

Manufacturing of the device comes with different challenges, mainly with deviation in height and width of the waveguides. This then results in deviations from the parameters with designed and manufactured components. For example, the height can vary from 215.3 nm to 223.1 nm although the designed height is 220 nm. Similarly there can be a variation of 470 nm to 510 nm in width although the designed value is 500 nm. Hence corner analysis is done to account for these variations. For example, the group index for 500x220 nm waveguide for a wavelength of 1550 nm, for TE can vary from 4.158 to 4.235. FSR variation for a ΔL of 100 µm for TE and TM mode is as shown in Table 1.

Mode	FSR min	FSR max
TE	5.65	5.76
TM	6.25	6.88

Table 1. Minimum and Maximum FSR using Corner analysis

C. *Baseline Correction*

Baseline Correction is a method to remove the baseline shape of the grating couplers from the measurement data. This is because of the fact that grating couplers have a limited bandwidth which result in a curved amplitude response. The idea is to curve-fit the spectrum and then subtract this from the subsequent data. All the experiments have been conducted at room temperature of 25 deg Celsius.

Although the analysis has been done for all the MZI structures, for keeping the paper/report a concise one, only analysis wrt MZI-4 is considered in subsequent sections.

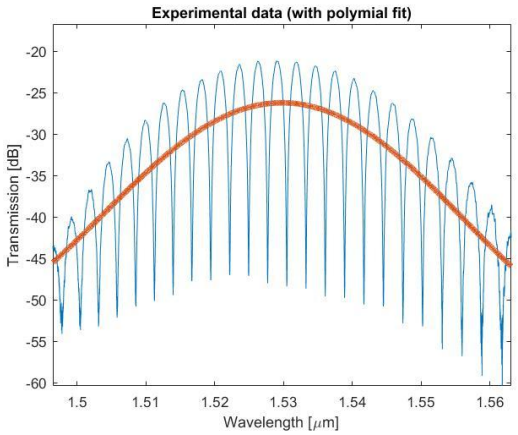

Fig. 10. Experimental Data with polynomial fit

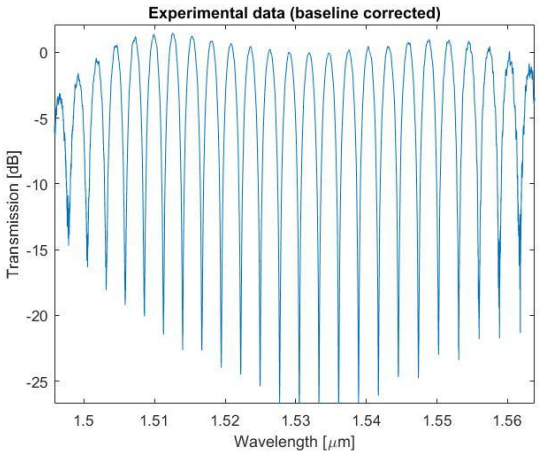

Fig. 11. Baseline Corrected data

D. *MZI transmit spectrum*

The transmission spectrum of MZI-4 and its curve fitted data is as shown in Fig 12. Group Index and FSR can be extracted during this process via MATLAB programming.

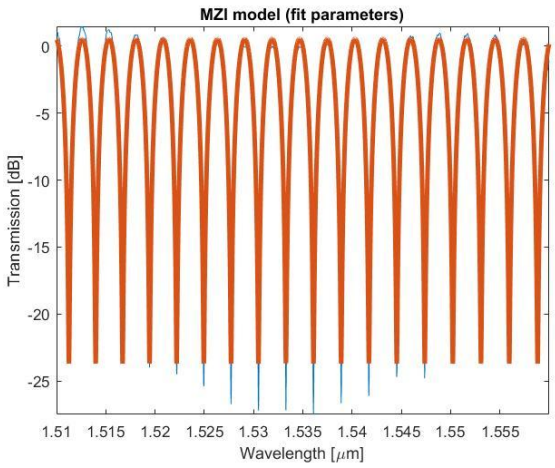

Fig. 12. Transmission spectrum of a MZI, blue curve: experimental data, red curve: curve fitted data.

The extracted group index values for TE devices are as shown in Table 2.

# Device	ΔL (μm)	ng	Goodness of Fit
Ref TE-1	-	-	-
MZI-2	38.52	4.1914	0.9892
MZI-3	74	4.1929	0.9893
MZI-4	200.6	4.1962	0.9863
MZI-5	200.6	4.1955	0.9872

Table 2. Group Index values for TE devices

The extracted group index values for TE devices are as shown in Table 3.

# Device	ΔL (μm)	ng	Goodness of Fit
Ref TM-1	-	-	-
MZI-7	174	3.8131	0.9963
MZI-8	253.2	3.8080	0.9978
MZI-9	327	3.8141	0.9974

Table 3. Group Index values for TM devices

IV. CONCLUSION

This paper focus on the modelling a Mach Zehnder Interferometer in commercially available standard simulation softwares like Lumerical, layout design using KLayout and then comparing the parameters like group index and actual fabricated device. Various techniques like corner analysis, curve fitting, autocorrelation are explored for the data analysis. The results obtained were within the limits of expected data.

ACKNOWLEDGMENT

I acknowledge Dr. Fredy Francis, for helping me out with fund related activities for this course. I also acknowledge edX UBCx Phot1x Silicon Photonics Design, Fabrication and Data Analysis course, which is supported by the Natural Sciences and Engineering Research Council of Canada (NSERC) Silicon Electronic-Photonic Integrated Circuits (SiEPIC) Program. Matteo Branion-Calles performed the measurements at The University of British Columbia. I acknowledge Applied Nanotools, Inc., Lumerical Solutions, Inc., Mathworks, Mentor Graphics, Python, and KLayout for the design software.

REFERENCES

[1] Xiangdong Li, Xue Feng, Kaiyu Cui, Fang Liu, and Yidong Huang, "Integrated silicon modulator based on microring array assisted MZI," Opt. Express, 2014

[2] Sung Joong Choo, Jinsik Kim, Kyung Woon Lee et Al, An integrated Mach–Zehnder interferometric biosensor with a silicon oxynitride waveguide by plasma-enhanced chemical vapor deposition, Current Applied Physics, Volume 14, Issue 7,2014

[3] Chen Zhu, Liangjun Lu, Wensheng Shan, Weihan Xu, Gangqiang Zhou, Linjie Zhou, and Jianping Chen, "Silicon integrated microwave photonic beam former," Optica 7,2020

[4] Lukas Chrostowski, Michael Hochberg, chapter 12 in "Silicon Photonics Design: From Devices to Systems", Cambridge University Press, 2015

[5] http://siepic.ubc.ca/probestation, using Python code developed by Michael Caverley.

[6] Yun Wang, Xu Wang, Jonas Flueckiger, Han Yun, Wei Shi, Richard Bojko, Nicolas A. F. Jaeger, Lukas Chrostowski, "Focusing sub-wavelength grating couplers with low back reflections for rapid prototyping of silicon photonic circuits", Optics Express Vol. 22, Issue 17, pp. 20652-20662 (2014) doi: 10.1364/OE.22.020652

[7] www.plcconnections.com, PLC Connections, Columbus OH, USA.

[8] http://mapleleafphotonics.com, Maple Leaf Photonics, Seattle WA, USA.